Shahrood University of Technology

Journal of Mining and Environment (JME)

Journal homepage: www.jme.shahroodut.ac.ir

Iranian Society of Mining Engineering (IRSME)

Estimation of Land Surface Temperature of Sahibzada Ajit Singh Nagar, Punjab, India

Kaustubh Sinha, Priyangi Sharma, Kanwarpreet Singh*, Sushindra Kumar Gupta, and Abhishek Sharma

Department of Civil Engineering, Chandigarh University, Gharuan, Punjab, India

Article Info

Received 5 April 2023
Received in Revised form 21 April 2023
Accepted 2 May 2023
Published online 2 May 2023

DOI:10.22044/jme.2023.12923.2344

Keywords

LST
NDVI
Brightness Temperature
PV
Specific Humidity

Abstract

Land surface temperature (LST) is one of the most important geological features of any area in the present times. During the study, the information regarding the land surface temperature is calculated using the Arc-GIS software. The LANDSAT 8 (2022) and LANDSAT 4-5 (2001 and 2011) satellite images are used for the calculation of LST. From the LST maps of years 2001 and 2011, a significant rise is noticed; this is due to the rapid increment in the population of the said area. A gradual increment in the LST is present between the second period of 2011-2022. A connection between the LST and the specific humidity has also been drawn in this aspect. The specific humidity in the region has seen a significant increment in the concerned time period. Overall, it is observed that the LST of the area has increased rapidly from the -12 ˚C minimum temperature in 2001 to 27 ˚C in 2022; this is because of the human activity in the area, which has ultimately catered towards the degradation of the climatic condition and environment like LST.

1. Introduction

The issue to Land Surface Temperature (LST) is a major problem with the changing climatic scenarios; this has been an issue for a long time. However, in the recent decades, with the population shooting up the reason of the increment in LST has majorly been the human activity. The unplanned and non-sustainable industrialization has contributed to all the mishaps related to climate change and this same has been hazardous for LST. Geographic information system (GIS) and RS have proved to be very significant in analyzing and assessing LULC changes as well as LST. Satellite-based RS has the ability to provide synoptic LST data at a specific time and location. LST can be applied for finding global warming, vegetation suitability, glacier, urban heat temperature monitoring, and many more. Landsat 8 with a payload of new instrument called the Thermal Infrared Sensors (TIRS) helps in better analysis of LST data [1]. LST is a key parameter for surface energy balance and urban climatology studies. LST is affected by the characteristics of the land surface such as vegetation cover and its type, land use-land cover, and surface imperviousness [2]. Remotely sensed thermal infrared (TIR) data has been widely used to retrieve LST. LST is an important parameter in the studies of urban thermal environment and dynamics [3]. The intensification of LST is a consequence of changes in land use land cover (LULC). Global urbanization has witnessed a significant increase over the past few decades. Although urbanization is a common phenomenon around the world, it has become more intense and dynamic in developing countries because of rapid economic growth [4]. Urbanization leads to the construction of various urban infrastructures in the city area for residency, transportation, industry, and other purposes, which causes major land use change. Consequently, it substantially affects LST by unbalancing the surface energy budget. A higher LST in city areas decreases human thermal comfort for the city

Corresponding author: Kanwarpreet.e9570@cumail.in (S.K. Singh)

dwellers, and affects the urban environment and ecosystem. Therefore, a comprehensive investigation is required to evaluate the impact of land use change on the LST [5].

Extreme land-use and land-cover (LULC) as the result of rapid urbanization has been raising land surface temperature of core city areas and its surrounding. Therefore, investigation on surface temperature is very vital to analyze temperature variations and minimize its effect [6]. LST and UHI (urban heat island), directly associated with LU changes, are the parameters that should be considered in similar studies. Therefore, Remote Sensing (RS) and Geographic Information Systems (GIS) are commonly used to obtain this kind of information [7]. The soft computing models used for predicting LST changes are very useful to evaluate and forecast the rapidly changing climate of the world. Climate change is one of the most critical challenges that the world faces. Previous studies have reported that climate change has a significant effect on the LST [8]. Urban green space is one of the most essential components in contributing to ecological balance and environmental sustainability. Due to rapid urbanization in the last few decades, massive reduction of urban vegetation cover (VC) has increased the LST and hampered the environmental sustainability [9]. LST and vegetation cover changes are two indicators of landscapes in a region. The relationship between LST anomalies, elevation, vegetation, and urban growth is significant to conservation [10]. Spatial and temporal information on urban infrastructure is essential, and requires various land-cover/land-use planning and management applications. Besides, a change in infrastructure has a direct impact on other land-cover and climatic conditions [11]. Agricultural land conversion due to urbanization, industrialization, and many other factors is one of the significant concerns to food production. Therefore, analyzing the temporal and spatial variation of agricultural lands is an emerging topic in the research world [12].

Knowledge of the LST provides information on the temporal and spatial variations of the surface equilibrium state and is of fundamental importance in many applications. As such, the LST is widely used in a variety of fields including evapotranspiration, climate change, hydrological cycle, vegetation monitoring, urban climate, and environmental studies, among others, and has been recognized as one of the high-priority parameters of the International Geosphere and Biosphere Program (IGBP) [13]. The importance of LST for environmental studies has been highlighted by several authors. Various algorithms have been developed to retrieve LST from at-sensor and auxiliary data: single-channel methods, split-window technique and multi-angle methods. To apply the last two methods, at least two thermal channels are required. The estimation of LST with only one thermal channel is the main advantage for single-channel methods. For example, this is the only method that can be applied to the Landsat platform, with one thermal channel (Thematic Mapper, band 6). Traditionally, the main disadvantage of this method is that some atmospheric parameters are needed, usually by mean of a radio sounding [14]. Remote sensing of urban heat islands (UHIs) has traditionally used the Normalized Difference Vegetation Index (NDVI) as the indicator of vegetation abundance to estimate the (LST)–vegetation relationship. This study investigates the applicability of vegetation fraction derived from a spectral mixture model as an alternative indicator of vegetation abundance. This is based on examination of a Landsat Enhanced Thematic Mapper Plus (ETM+) image of Indianapolis City, IN, USA, acquired on June 22, 2002. The transformed ETM+ image was unmixed into three fraction images (green vegetation, dry soil, and shade) with a constrained least-square solution [15]. LST is defined as the temperature felt when the land surface is touched with the hands or the skin temperature of the ground. As one of the most important aspects of the land surface, LST has been a main topic for developing methodologies to be measured from space. LST is an important factor in many areas of studies such as global climate change, hydrological and agricultural processes, and urban land use/land cover. Calculating LST from remote sensed images is needed since it is an important factor controlling most physical, chemical, and biological processes of the Earth. There is a growing awareness among environmental scientists that remote sensing can and must play a role in providing the data needed to assess ecosystems conditions and to monitor change at all special scales. The tool developed in this paper is simple and does not require any background knowledge, so scientists can use it very easy in their research works [16]. LST is a very important parameter in the surface process of land-air interaction. Due to their very high spatial resolution, the thermal band data of the Landsat series such as the Landsat 5 Thematic Mapper (TM) and the Landsat 7 Enhanced Thematic Mapper (ETM) have been widely applied for LST retrieval for such studies as surface energy budget

estimation, surface moisture and evapotranspiration monitoring, urban heat island monitoring and environmental biogeochemistry process simulation, requiring LST as a basic input. The Landsat 8 thermal infrared (TIR) instrument designed with two TIR bands is very suitable for the split-window algorithm for LST retrieval, for Landsat 8 Thermal Infrared Sensor (TIRS) data the single-channel (SC) algorithms and split-window algorithms to Landsat 8 TIRS data for LST retrieval. However, several artifacts including banding and absolute calibration discrepancies that violate the requirements in some scenes had been observed in the TIRS data [17]. The importance of LST retrieved from high to medium spatial resolution remote sensing data for many environmental studies, particularly the applications related to water resources management over agricultural sites, was a key factor for the final decision of including a thermal infrared (TIR) instrument on board the Landsat Data Continuity Mission or Landsat-8. This new TIR sensor (TIRS) includes two TIR bands in the atmospheric window between 10 and 12 μm, thus allowing the application of split-window (SW) algorithms in addition to single-channel (SC) algorithms or direct inversions of the radiative transfer equation used in previous sensors on board the Landsat platforms, with only one TIR band [18]. A large number of water- and climate-related applications such as drought monitoring are based on spaceborne-derived relationships between LST and the normalized difference vegetation index (NDVI). The majority of these applications rely on the existence of a negative slope between the two variables, as identified in site- and time-specific studies. The current paper investigates the generality of the LST–NDVI relationship over a wide range of moisture and climatic/radiation regimes encountered over the North American continent (up to 60°N) during the summer growing season (April–September). Information on LST and NDVI was obtained from long-term (21 years) datasets acquired with the Advanced Very High-Resolution Radiometer (AVHRR). It was found that when water is the limiting factor for vegetation growth, the LST–NDVI correlation is negative [19]. LST and normalized difference vegetation index (NDVI) were computed based on LULC types. The results show that agricultural land decreased, while urban areas expanded dramatically, and forest land increased slightly. Barren land increased from 1991 to 1994, and then decreased from 1994 to 2001. These changes in LULC widened the temperature difference between the urban and the rural areas. The change in LST was mainly associated with changes in construction materials in the urban area and in vegetation abundance both in the urban and rural areas. Vegetation had a dual function in the temperatures of different LULC types. While it could ease the warming trend in the urban or built-up areas, it helped to keep other lands warmer in the cold weather. The study also reveals that due to the government's efforts on reforestation, rural ecosystems in some of the studied area were being restored. The time required for the karst ecosystem to recover was shorter than previously thought [20]. LST can be defined as the temperature felt when the land surface is touched with the hands or it is the skin temperature of the ground. LST is the temperature emitted by the surface and measured in kelvin. It was greatly affected by the increasing green house gases in the atmosphere. As it rises, it melts the glaciers and ices sheets in the polar region. Thus it leads to flood and sea level rise. Increase in LST also affects the climatic condition of the monsoon countries leading to unpredictable rainfall. The vegetation in the entire Earth surface will be affected by this. Land use/Land cover (LU/LC) of an area can be used for estimating the amount of LST. The natural and anthropogenic activities change the LU/LC of an area. This also influences LST of that area. As its value changes the local climate of the area also changes. It is an important phenomenon to be investigated. Hence, many researchers had calculated LST using various algorithms and techniques [21].

In this research work, we analyse the variations in LST patterns in the district Sahibzada Ajit Singh Nagar. The main objectives of this research work are to generate decade-wise LST maps for the studied area from 2001 to 2022, and to perform a comparative analysis of the data across each decade. LST is one of the most important parameters in the physical processes of surface energy and water balance at local through global scales.

2. Materials and methodology

2.1. Studied area

The research was conducted in the Mohali region, also referred to as SAS Nagar, an important city adjacent to the Union Territory of Chandigarh. Mohali, officially known as Sahibzada Ajit Singh Nagar, is a well-planned city located in the Mohali district of Punjab, India. It serves as both an administrative and commercial hub, situated

southwest of Chandigarh. The area falls in the survey of India Toposheet, which lies between 30°21'00" and 30°56'00" North latitude and 760 30' to 760 55' East longitude covering an area of 1189 sq km, as shown in Figure 1. The average temperature variation of this area is quite stable. The temperature in summer may rise to a maximum of 47 °C (117 °F). Temperatures generally remain between 30 and 40 °C (86 and 104 °F). In autumn, the temperature may rise to a maximum of 36 °C (97 °F). Temperatures usually remain between 16 and 27 °C (61 and 81 °F) in autumn. The minimum temperature is around 13 °C (55 °F). Average temperatures in winter (November to February) remain at (maximum) 7 to 15 °C (45 to 59 °F) and (minimum) 1 and 5 °C (34 and 41 °F). Spring temperatures vary between (min) 16 and 25 °C (61 and 77 °F) (max). The population of the district is 9,94,628, as per 2011 census. The total rural population is 544611 (59.74%) and the urban population is 450017 (40.26%) and the decennial growth rate is 30.02 % (2001-2011). Population density of district is 830 persons/sq. km. Population density of district is 830 persons/sq. km. Mohali has a sex ratio of 879 females for every 1000 males and literacy rate of 83.80%. The temperature ranges from 40.40 C (May/June) to 7.10 C (December/January) and maximum temperature was observed is 470C. The average annual rainfall is 617 mm, and Normal Annual rainfall is 1061, respectively, which is unevenly distributed over the area 49 days Monsoon rainfall contributes 70% of annual rainfall in the district. The rainfall increases from southwest to northeast in the district. For past 30 years the population of SAS Nagar specially between the period of 2001 and 2011 (from 7.47 lakhs to 9.95 lakhs). This has contributed in extensive unsustainable industrialization increasing negative climatic actions.

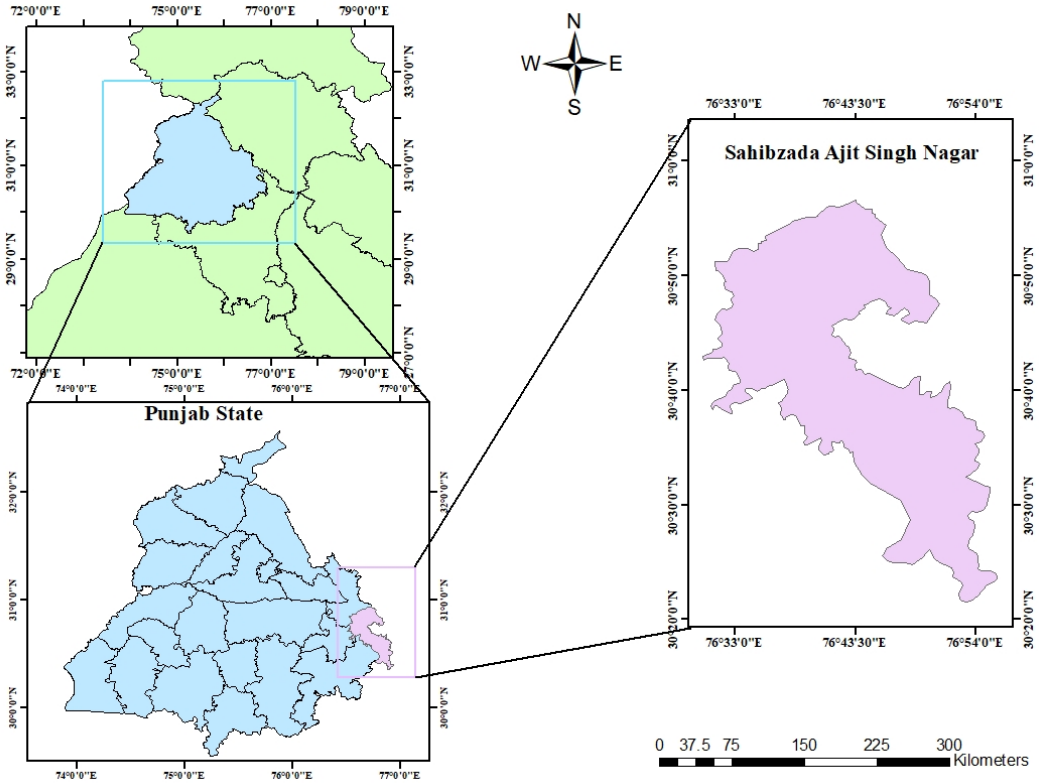

Figure 1. Map of studied area.

2.2. Data collection

2.2.1. For LST

LST different satellite images have been downloaded from USGS platform. The satellite bands LANDSAT4-5 and LANDSAT 8 (OLI and TIRS). The data acquired is listed in Table 1 along with the date of production, resolution, and source.

Table 1. Data source.

Sl. No.	Source	Year	Date	Satellite
1.	USGS Earth Explorer	2001	16/03/2001	LANDSAT 4-5
2.	USGS Earth Explorer	2011	20/09/2011	LANDSAT 4-5
3.	USGS Earth Explorer	2022	06/06/2022	LANDSAT 8

2.2.2. For specific humidity

Data collection for the specific humidity was done using NASA Power Dataset. In this, we put up 20 latitudes and longitude points and extracted the data for each point for specific humidity for years 2001, 2011, and 2022.

2.3. Proposed methodology of LST estimation

The LST of the studied area was determined using a variety of methods. These methods included extracting Satellite Band Images for the years 2001, 2011, and 2022 from the USGS Earth Explorer database. Afterward, the Raster Calculator tool of ArcGIS (ESRI) was utilized to perform calculations separately for each year. LANDSAT 4-5 imagery was used for the years 2001 and 2011, while LANDSAT 8 was used for the year 2022. The satellite band used for 2001 was dated 16/03/2001, while the one used for 2011 was dated 20/09/2011, as shown in Figure 2. The Raster Calculator tool of Arc-GIS was used to apply the necessary calculations to the satellite image. For conversion of DN to radiance is given as in Equation (1).

$$L\lambda = \left(\frac{L_{max} - L_{min}}{Q_{calmax} - Q_{calmin}}\right) * (Q_{cal} - Q_{calmin}) + L_{min} \quad (1)$$

where Lλ = spectral radiance, cal = Quantized and calibrated standard product pixel values (BAND 6), L_{MAX} = spectral radiance that is scaled to $Qcal_{MAX}$ (15.303 for Landsat 4-5), L_{MIN} = spectral radiance that is scaled to Qcalmin (1.238 for Landsat4-5), Qcalmax = maximum quantized calibrated pixel value (255), Qcalmin = minimum quantized calibrated pixel value (1). Mathematically for estimation of LST is express in Equation (2).

$$T = \left(\frac{K2}{\ln\left(\frac{K1}{L}\right) + 1}\right) - 273.15 \quad (2)$$

where T = Effective satellite temperature in Kelvin, K_i = Calibration Constant 1 (607.76 for Landsat 4-5), K_{ii} = Calibration Constant 2 (1260.56 for Landsat 4-5).

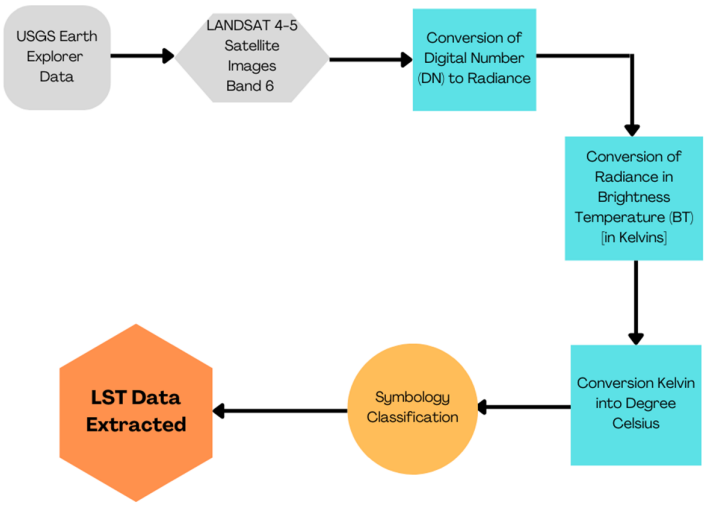

Figure 2. LST data extraction process for LANDSAT 4-5.

2.3.2. For LANDSAT 8 (Year 2022)

2.3.2.1. Spectral radiance conversion from digital number (DN)

When the earth's surface temperature rises over absolute zero, it generates electromagnetic thermal energy (Kelvin). The thermal sensors on the satellite sensors receive this electromagnetic heat energy and store it as digital numbers (DNs). Using the following equation, convert this DNs to At Sensor Spectral Radiance with the necessary constant. Adopting the radiance rescaling factor, TOA (top of atmosphere) spectral radiance can be obtained by converting from thermal infra-red. Spectral radiance can be denoted by "Lλ".

$$L\lambda = ML \times Q_{cal} + AL - Di \quad (3)$$

where Lλ = TOA, spectral radiance = radiance multiplicative band, ML = 0.0003342 (LANDSAT 8 OLI & TIRS), AL = Radiance Add Band, AL = 0.10000, Qcal = Quantized and calibrated standard product pixel values (BAND 10), Di = 0.29. The second step is to convert the spectral radiance into Brightness Temperature (BT) from TOA spectral radiance in Celsius using the following conversion formula:

$$BT = \frac{K2}{ln\left(\frac{K1}{L\lambda} + 1\right)} - 273.15 \quad (4)$$

where K1 = thermal conversion constant (774.8853) and K2 = thermal conversion constant (1321.0789). NDVI detects the vegetation cover of the region of interest, and is calculated using BAND-4 and BAND-5 of Landsat-8 images using the equations. Mathematically, NDVI as expressed in Equation (5).

$$NDVI = \frac{(Band5 - Band4)}{Band5 + Band4} \quad (5)$$

The proportion of vegetation (PV), which is immensely correlated to the NDVI, and emissivity (ε), must both be computed after the NDVI is calculated. For estimation of Proportion of Vegetation (PV) is given in Equation (6).

$$PV = Square\left\{\frac{NDVI - NDVI_{min}}{NDVI_{max} - NDVI_{min}}\right\} \quad (6)$$

The minimum and maximum values of an NDVI image are usually displayed directly in the image in Arc-GIS; otherwise, the values must be obtained by accessing the raster's attributes. Mathematically, for estimation of Land Surface Emissivity (ε) as given in Equation (7).

$$\varepsilon = 0.004 \times PV + 0.986 \quad \textbf{(7)}$$

0.986 corresponds to a correction value of the equation. For assessment of LST value is expressed in Equation (8).

$$LST = \frac{BT}{1 + \left(\lambda * \frac{BT}{C2}\right) * \ln(\varepsilon)} \quad (8)$$

where C2 = 14388, the detailed methodology of LST Data Extraction Process for LANDSAT 8, as given below in Figure 3.

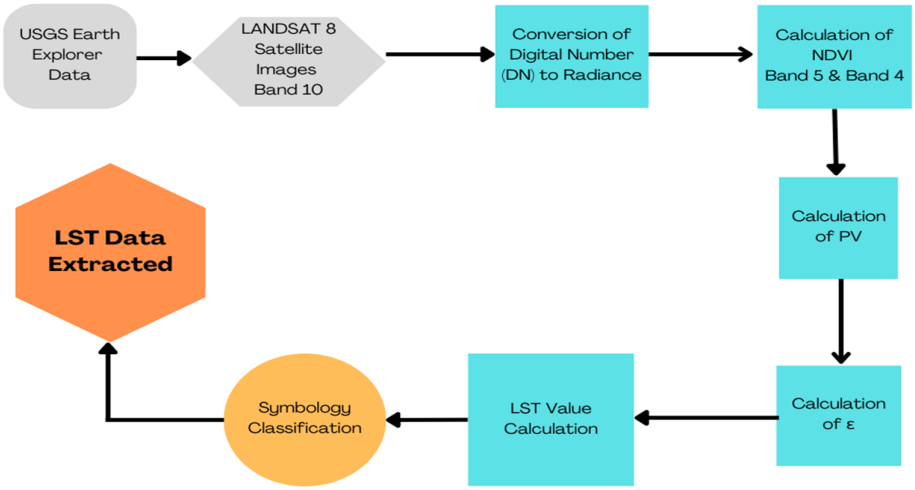

Figure 3. Detailed methodology of LST data extraction process for LANDSAT 8.

2.3.3. Estimation of specific humidity (SH)

Similar to the process used for extracting LST data, specific humidity data was also obtained through several steps. Initially, the latitude and longitude of the studied area were extracted and then used to download specific humidity data from

the NASA Power Dataset. Once the data for all three years was downloaded, the coordinates were inputted into Arc-GIS (ESRI) software, and the Inverse Distance Weighted (IDW) tool was used on the data, as depicted in Figure 4. IDW is an interpolation method that enables the mapping of data on multiple variables (coordinates) within a studied area. This interpolation method is highly accurate since the data is compiled before mapping. A total of twenty (20) coordinate sets were compiled from various satellite stations.

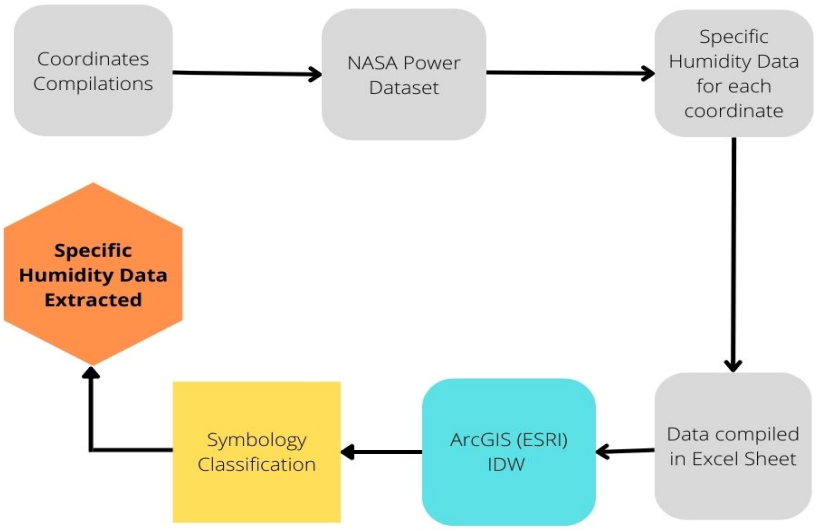

Figure 4. Detailed methodology of specific humidity data extraction process.

3. Results and Discussion

3.1. LST

To analyze the temperature changes, the spectral data has been divided into 5 temperature ranges in each map (2001, 2011, and 2022). These classifications have been done on the by rounding of the given data up to 2 significant figures. The units incorporated in the study are in degrees Celsius. For the year 2001, The temperature ranges, expressed in degrees Celsius, are divided into five intervals: from -12 to -5.3, from -5.2 to 0.88, from 0.89 to 7.9, from 8 to 16, and from 17 to 27. The same temperature ranges were observed for the year 2011, which were: 22 to 25, 26 to 27, 27 to 28, 28 to 29, and 29 to 34 degrees Celsius. Similarly, for the year 2022, the temperature ranges were 27 to 37, 38 to 39, 40 to 41, 42 to 43, and 44 to 49 degrees Celsius. These temperature ranges are shown in Figure 5. The data given significantly establishes the fact that over the year, the LST of the region (studied area) has risen. Where it was around -12 ˚C in 2001 as its minimum temperature, in 2022 it is 27 ˚C. This change shows that the rapid increase in various environmental hazardous factors have catered to the cause of rising the LST significantly. It is evident that there is a significant difference in Land surface temperature variation between the years 2001 and 2011, as compared to 2011 and 2022, as shown in Figure 6. This indicates that there was a greater level of environmental risk during the former period. In addition to natural environmental threats, human factors such as population growth and rapid and unsustainable development have contributed to the increase in land surface temperature in the area.

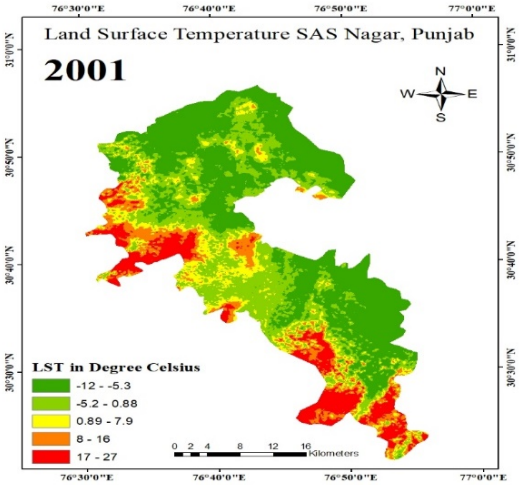

a) LST 2001

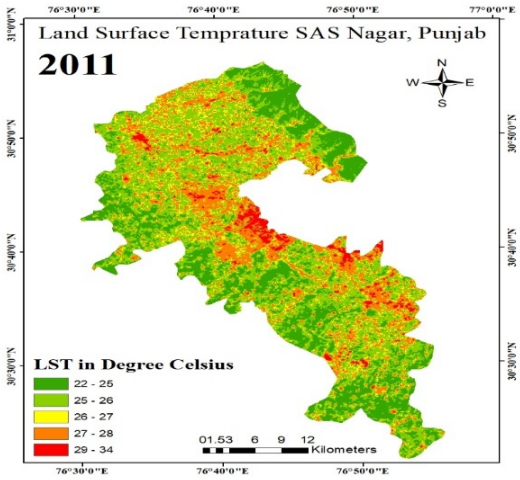

b) LST 2011

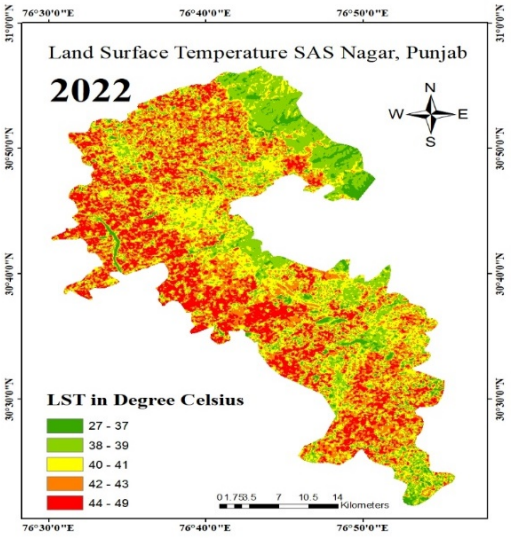

c) LST 2022

Figure 5. LST of last two decades.

LST is an important feature of any region. The correlation of LST can be done with many other physical features, like specific humidity. The LST plays an important role in the economic value of any region too, with change in the LST the possibilities of change in the soil quality and its crop favoring nature might also change as LST directly effects the water table in the region. The decrement of ground water, change in the soil feature and the crop production all these cater to a hazardous effect on the economic development in the region, things tend to fall out of order in regions with low agricultural produce given the case that majority of Indian economy is agriculture driven. The changes in the population affects any region in the world, with drastic climatic change all around the world, increase in human population and not much of the betterment in the environmental conditions caters to many ill effects. As previously noted, the economic decline in the region caused by the soil's inability to support crop production will inevitably lead to inflation, particularly in regions such as Punjab that heavily rely on the agricultural economy. Punjab is a major player in the Indian agriculture market.

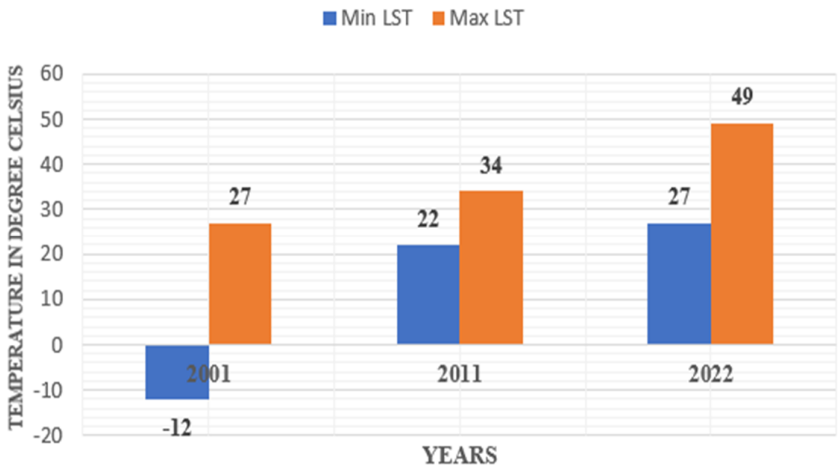

Figure 6. LST comparison of SAS, Nagar.

With the passage of time, the lowest and the highest LSTs have changed drastically. The temperature in 2022 has shown a significant increase compared to 2001, where the lowest temperature of -12 ˚C has now risen to 27 ˚C. A similar trend is observed in the maximum temperature as well. In 2001, the maximum LST was 27 ˚C, which increased to 34 ˚C in 2011 and further spiked to 49 ˚C in 2022. These details are presented in Table 2 and Figure 7, and are illustrated in the graph.

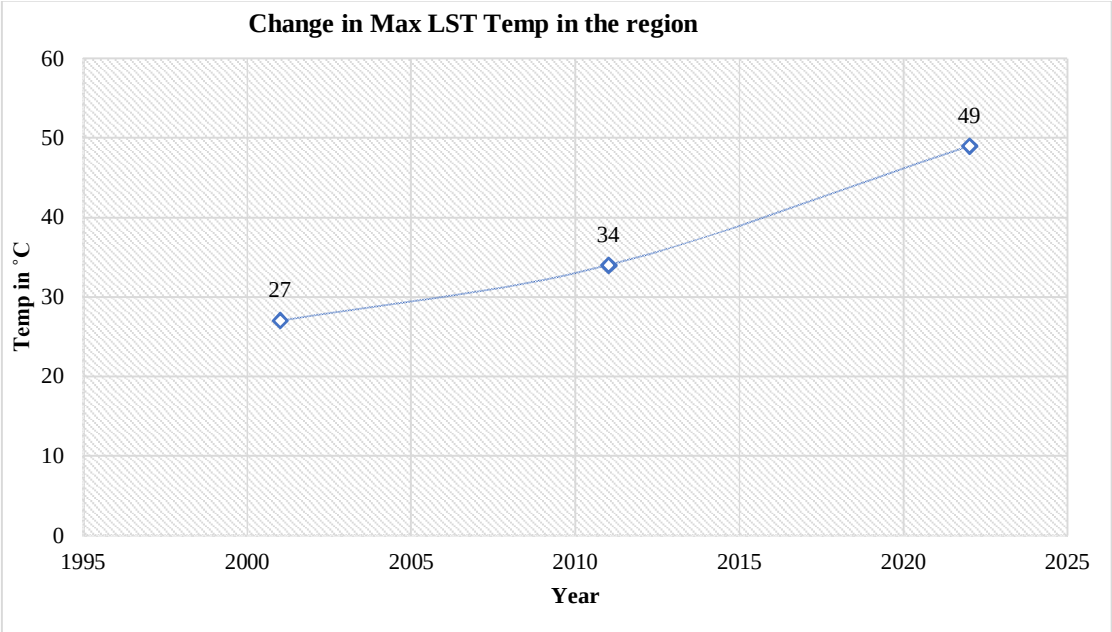

Figure 7. Change in Max LST Temp in the region.

3.2. LST range comparison

Table 2 displays the LST variations observed in the studied region over the course of three years: 2001, 2011, and 2022.

According to Table 2, the greatest percentage of area (42.5%) is found in the coldest temperature range (-12 to -5.3 ˚C). As the temperature range increases, the percentage area gradually decreases, with the lowest percentage found in the 8-16˚C range. This information is visually represented in the accompanying graph.

Table 2. LST range for 2001, 2011, and 2022 years.

SI. No	Year	Temp. range (˚C)	Percentage area
1		From -12 to -5.3	42.5
2		From -5.2 to 0.88	26.7
3	2001	From 0.89 to 7.9	11.0
4		From 8 to 16	9.8
5		From 17 to 27	10.0
6		From 22 to 25	23.6
7		From 25 to 26	39.9
8	2011	From 26 to 27	12.5
9		From 27 to 28	20.9
10		From 29 to 34	3.1
11		From 27 to 37	4.4
12		From 38 to 39	19.8
13	2022	From 40 to 41	28.2
14		From 42 to 43	28.5
15		From 44 to 49	19.1

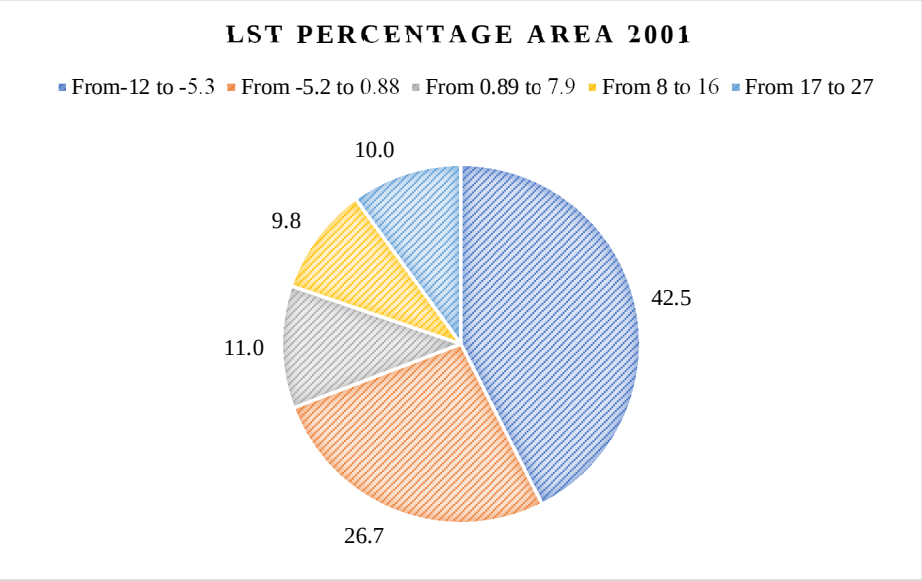

Figure 8. LST range percentage area 2001.

According to Figures 8 and 9, the proportion of the lowest range in terms of area decreased by about 50% between 2001 and 2011. Specifically, it dropped from 42.5% in 2001 to 23.6% in 2011. This significant decline may be attributed to the population increase in the region during the 10-year period from 2001 to 2011.

In the year 2022, the observation explains that the highest area is covered during the temperature range of 42-43 ˚C, i.e. 28.5%, as mentioned in Figure 10.

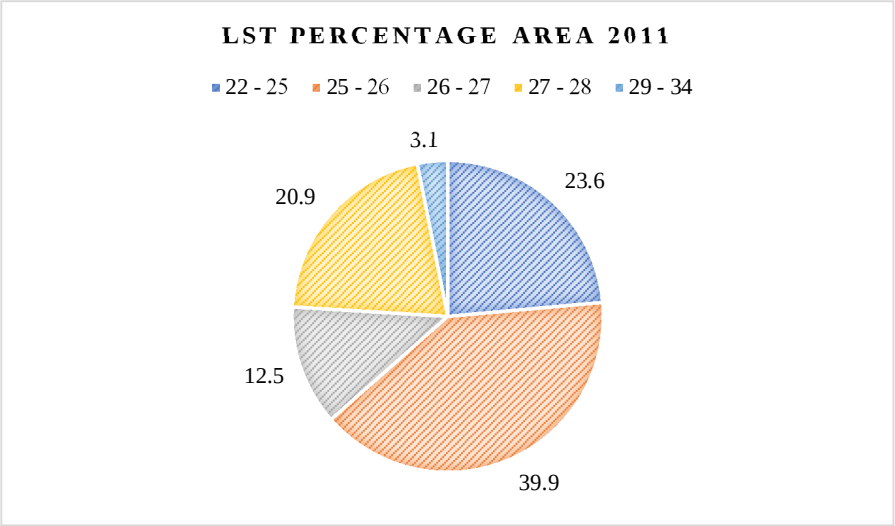

Figure 9. LST range percentage area 2011.

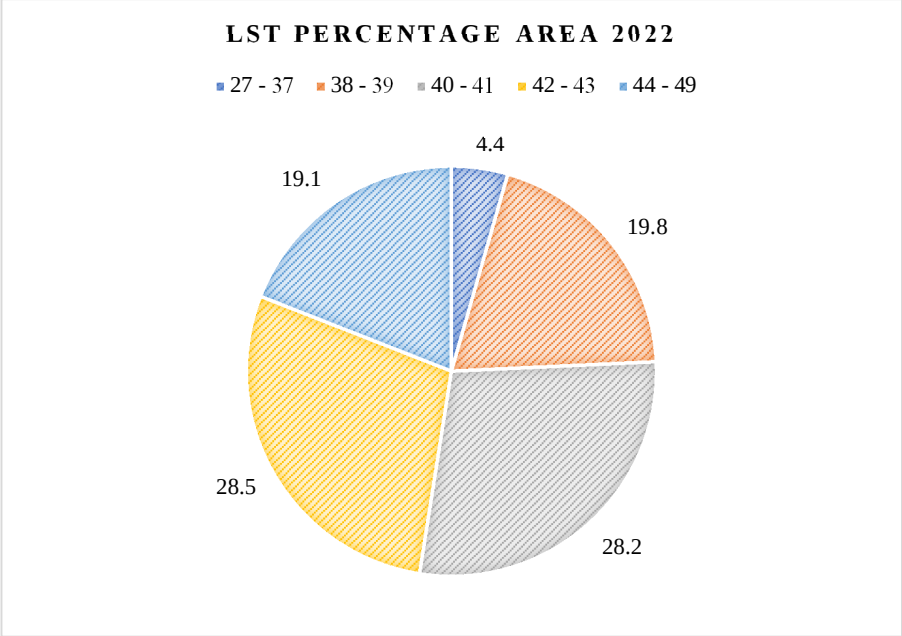

Figure 10. LST range percentage area 2022.

3.3. Specific humidity

Just as specific humidity is linked to LST, spectral data has also been categorized into 5 ranges to enhance comprehension. The data has been expressed in the g/kg unit, as specified in the NASA Power Dataset. The correlation between specific humidity and the data was established due to the recognized correlation between temperature and humidity, which was also applied here. The classification for the data has been done uniformly throughout all three study years that are, 2001, 2011, and 2022, as given in Figure 11. The changes in the maps of specific humidity are similar to that observed in the LST. In 2001, the ranges were: 8.24 to 8.362, 8.363 to 8.484, 8.485 to 8.606, 8.607 to 8.728, and 8.720 to 8.85. In 2011, the ranges were: 9.77 to 9.94, 9.941 to 10.11, 10.12 to 10.28, 10.29 to 10.45, and 10.46 to 10.62. For the year 2022, the ranges were: 9.89 to 10.02, 10.03 to 10.16, 10.17 to 10.29, 10.3 to 10.43, and 10.44 to 10.56. This information can be seen in Figure 12 and Figure 13. Specific humidity shows a similar pattern to LST, and the comparison is presented graphically.

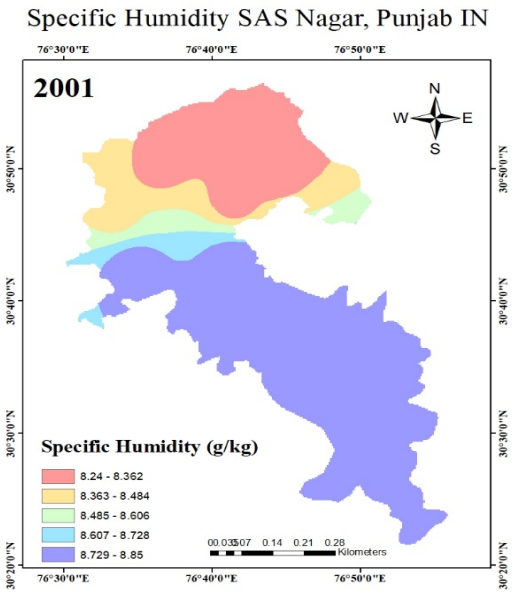

a). Specific humidity, 2001.

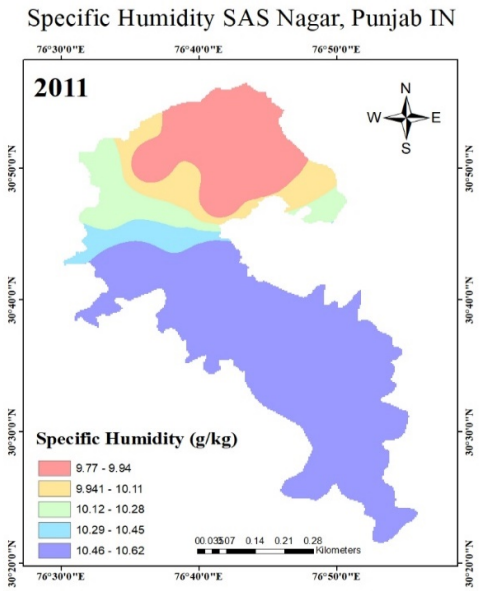

b). Specific humidity, 2011.

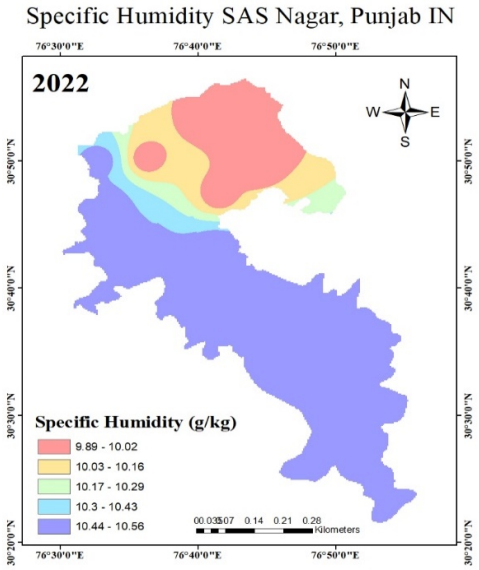

c). Specific humidity, 2022.

Figure 11. Comparison of specific humidity of proposed studied area.

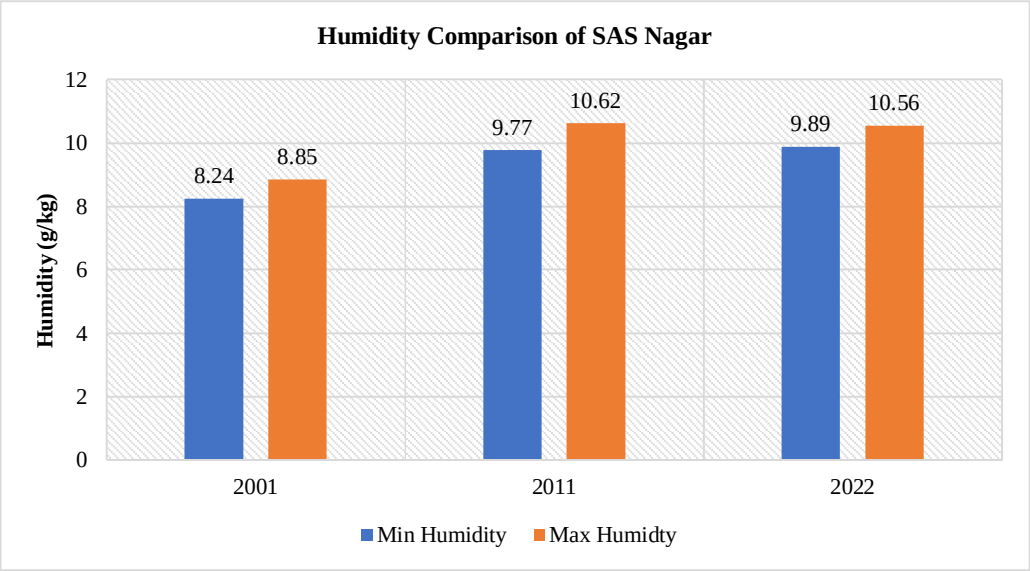

Figure 12. Comparison of minimum and maximum specific humidity of the proposed studied area.

The sole contrast that was observed between LST and specific humidity is that during the timeframe of 2011 to 2022, the maximum temperature of LST continued to rise annually, while the maximum specific humidity decreased slightly by 0.06. This information is visually depicted in the graph below, illustrating the same.

3.4. Relation of population and LST

Research has shown that urbanization often leads to an increase in non-sustainable industrialization, which can have negative impacts on the environment. This is due to the fact that human activity tends to increase in urban areas, which can lead to pollution and other environmental issues. In the case of Sahibzada Ajit Singh Nagar, there has been a significant increase in population over time. This population growth may have contributed to an increase in industrial activity, which could be impacting the environment in various ways. It is important to carefully monitor and manage urbanization and industrialization in order to minimize negative environmental impacts and promote sustainability in the long-term.

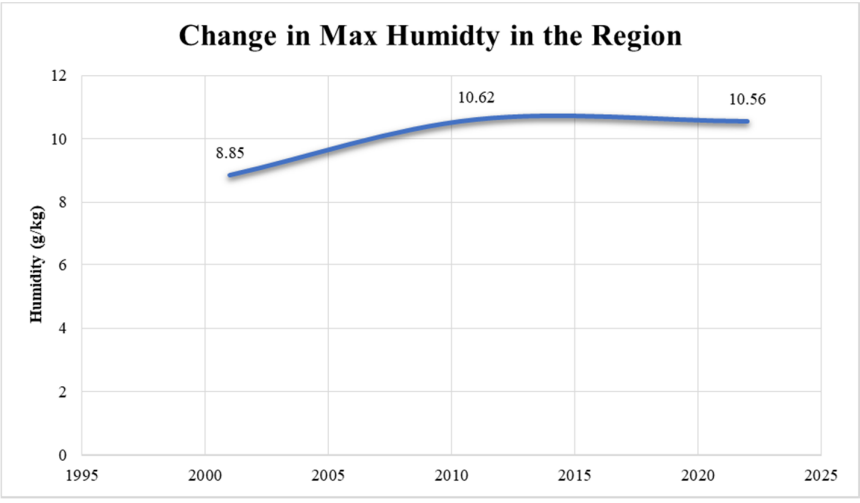

Figure 13. Change in Max Humidity in the region.

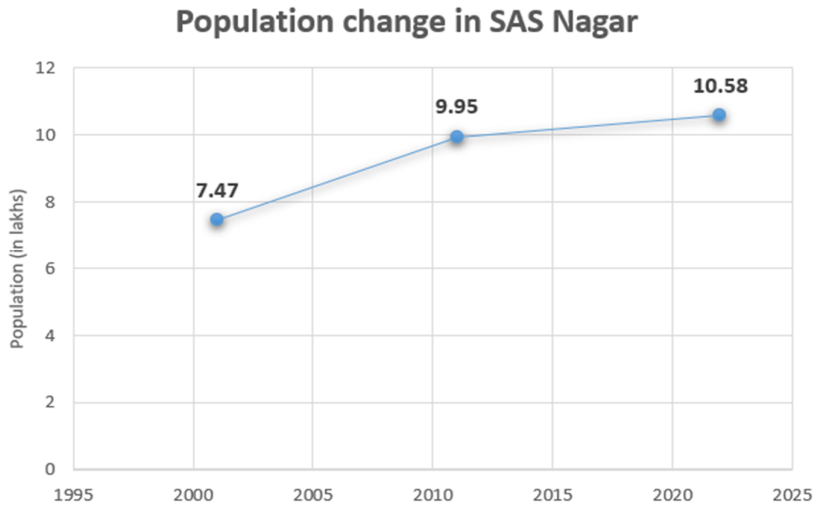

Figure 14. Change in population in SAS Nagar.

The relationship between population growth and LST can be observed through a reduction in the proportion of the region with the lowest LST range when comparing data from 2001, 2011, and 2022. This is illustrated in Figures 14 and 15, which provide a clear representation of this concept.

It can be noticed that when the population increased rapidly between the period of 2001 to 2011 the percentage area in the lowest range slashed approximately to half and this pattern continued further too. The alarming sight of increase in population and subsequently increment of LST can lead to extreme environmental hazards.

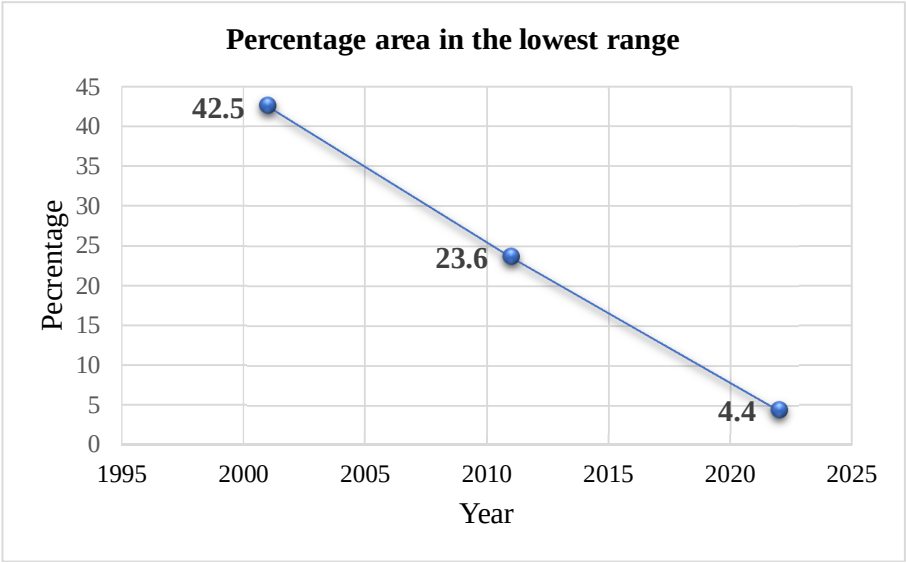

Figure 15. Comparison for percentage area in lowest range of LST.

4. Conclusions

The following conclusions can be drawn from the present study:

1. This study utilized satellite remote sensing and GIS, which offered a cost-effective and time-efficient approach for analyzing geographic data. The research's objective was to effectively communicate geographical data through the use of suitable symbols, and the map design must prioritize precise data presentation that aligns with actual geographic features. The maps presented in this research utilized land surface temperature (LST) mapping for three different years: 2001, 2011, and 2022. Analyzing LST mapping helped us identify changes in processes such as specific humidity between land surfaces and the atmosphere, which can impact the growth

rate and timing of various plants during different periods.

2. The analysis has told us that by the passage of time the LST of the studied area has shot up to such an extent that the maximus LST is approx. 49 ˚C, which was once just 27 ˚C in 2001. There are multiple reasons for the shift in LST but the primary factor is the increase in population within the area. Climate change is an extremely pressing issue globally, with research indicating a noteworthy impact on the land surface temperature as well as other related aspects. The expansion of urban areas is considered a significant factor for the change in land use and land surface temperature.
3. The correlation between LST and specific humidity indicates how strongly the characteristics of a region's physical environment are associated with LST. The rise in specific humidity exhibits a similar trend to that of LST, with both factors being connected to a significant increase in population in the study area. However, it is important to note that this information has been restated in a way that is not identical to the original text but retains its meaning.
4. Human activity has played a significant role in the global climate degradation, and the primary reason for it can also be attributed to human activity. The unsustainable industrialization aimed at meeting the needs of a rapidly increasing population has contributed to the adverse effects on the environment. All along these three years, 2001, 2010, and 2022, the industrialization in the entire state of Punjab has multiplied many folds, these industrialization, human activity contributed towards this degradation.

References

[1]. Singh, V. (2017). Estimating land surface temperature in ArcGIS using Landsat-8, Hoshangabad district, (Madhya Pradesh). IJAR, 3 (6): 1374-1379.

[2]. Khandelwal, S., Goyal, R., Kaul, N., and Mathew, A. (2018). Assessment of land surface temperature variation due to change in elevation of area surrounding Jaipur, India. The Egyptian Journal of Remote Sensing and Space Science, 21 (1): 87-94.

[3]. Malik, M.S. and Shukla, J.P. (2018). Retrieving of land surface temperature using thermal remote sensing and GIS techniques in Kandaihimmat watershed, Hoshangabad, Madhya Pradesh. Journal of the Geological Society of India, 92 (3): 298-304.

[4]. Dawid, W. and Bielecka, E. (2022). GIS-based Land Cover Analysis and Prediction based on Open-Source Software and Data. Quaestiones Geographicae. Vol. 41 (3): 75-86.

[5]. Imran, H.M., Hossain, A., Islam, A.S., Rahman, A., Bhuiyan, M.A.E., Paul, S., and Alam, A. (2021). Impact of land cover changes on land surface temperature and human thermal comfort in Dhaka city of Bangladesh. Earth Systems and Environment, 5, 667-693.

[6]. Traore, M., Lee, M.S., Rasul, A., and Balew, A. (2021). Assessment of land use/land cover changes and their impacts on land surface temperature in Bangui (the capital of Central African Republic). Environmental Challenges, 4, 100114.

[7]. Karakuş, C.B. (2019). The impact of land use/land cover (LULC) changes on land surface temperature in Sivas City Center and its surroundings and assessment of Urban Heat Island. Asia-Pacific Journal of Atmospheric Sciences, 55 (4): 669-684.

[8]. Mustafa, E.K., Co, Y., Liu, G., Kaloop, M.R., Beshr, A.A., Zarzoura, F., and Sadek, M. (2020). Study for predicting land surface temperature (LST) using landsat data: a comparison of four algorithms. Advances in Civil Engineering, 2020.

[9]. Kafy, A.A., Al Rakib, A., Akter, K.S., Rahaman, Z.A., Mallik, S., Nasher, N.R., and Ali, M.Y. (2021). Monitoring the effects of vegetation cover losses on land surface temperature dynamics using geospatial approach in Rajshahi city, Bangladesh. Environmental Challenges, 4, 100187.

[10]. Jamali, A.A., Kalkhajeh, R.G., Randhir, T.O., and He, S. (2022). Modeling relationship between land surface temperature anomaly and environmental factors using GEE and Giovanni. Journal of Environmental Management, 302, 113970.

[11]. Islam, S.U., Jan, S., Waheed, A., Mehmood, G., Zareei, M., and Alanazi, F. (2022). Land-cover classification and its impact on Peshawar's land surface temperature using remote sensing J. Computers, Materials and Continua, 70, 4123-45.

[12]. Makumbura, R.K., Samarasinghe, J., and Rathnayake, U. (2022). Multidecadal Land Use Patterns and Land Surface Temperature Variation in Sri Lanka. Applied and Environmental Soil Science, 2022.

[13]. Li, Z. L., Tang, B.H., Wu, H., Ren, H., Yan, G., Wan, Z., and Sobrino, J.A. (2013). Satellite-derived land surface temperature: Current status and perspectives. Remote sensing of environment, 131, 14-37.

[14]. Jiménez-Muñoz, J.C. and Sobrino, J.A. (2003). A generalized single-channel method for retrieving land surface temperature from remote sensing data. Journal of geophysical research: atmospheres, 108(D22).

[15]. Weng, Q., Lu, D., and Schubring, J. (2004). Estimation of land surface temperature–vegetation abundance relationship for urban heat island studies. Remote sensing of Environment, 89 (4): 467-483.

[16]. Avdan, U. and Jovanovska, G. (2016). Algorithm for automated mapping of land surface temperature using LANDSAT 8 satellite data. Journal of sensors, 2016.

[17]. Wang, F., Qin, Z., Song, C., Tu, L., Karnieli, A., and Zhao, S. (2015). An improved mono-window algorithm for land surface temperature retrieval from Landsat 8 thermal infrared sensor data. Remote sensing, 7 (4): 4268-4289.

[18]. Jiménez-Muñoz, J.C., Sobrino, J.A., Skoković, D., Mattar, C., and Cristobal, J. (2014). Land surface temperature retrieval methods from Landsat-8 thermal infrared sensor data. IEEE Geoscience and remote sensing letters, 11 (10): 1840-1843.

[19]. Karnieli, A., Agam, N., Pinker, R.T., Anderson, M., Imhoff, M.L., Gutman, G.G., and Goldberg, A. (2010). Use of NDVI and land surface temperature for drought assessment: Merits and limitations. Journal of climate, 23 (3): 618-633.

[20]. Xiao, H. and Weng, Q. (2007). The impact of land use and land cover changes on land surface temperature in a karst area of China. Journal of environmental management, 85 (1): 245-257.

[21]. Rajeshwari, A. and Mani, N.D. (2014). Estimation of land surface temperature of Dindigul district using Landsat 8 data. International Journal of Research in Engineering and Technology.

[22]. Amiri, R., Weng, Q., Alimohammadi, A., and Alavipanah, S. K. (2009). Spatial–temporal dynamics of land surface temperature in relation to fractional vegetation cover and land use/cover in the Tabriz urban area, Iran. Remote sensing of environment, 113 (12): 2606-2617.

[23]. Zhibin, R., Haifeng, Z., Xingyuan, H., Dan, Z., and Xingyang, Y. (2015). Estimation of the relationship between urban vegetation configuration and land surface temperature with remote sensing. Journal of the Indian Society of Remote Sensing, 43 (1): 89-100.

[24]. Choudhury, D., Das, K., and Das, A. (2019). Assessment of land use land cover changes and its impact on variations of land surface temperature in Asansol-Durgapur Development Region. The Egyptian Journal of Remote Sensing and Space Science, 22 (2): 203-218.

[25]. Dash, P., Göttsche, F.M., Olesen, F. S., and Fischer, H. (2002). Land surface temperature and emissivity estimation from passive sensor data: Theory and practice-current trends. International Journal of remote sensing, 23 (13): 2563-2594.

[26]. Edan, M.H., Maarouf, R.M., and Hasson, J. (2021). Predicting the impacts of land use/land cover change on land surface temperature using remote sensing approach in Al Kut, Iraq. Physics and Chemistry of the Earth, Parts A/B/C, 123, 103012.

[27]. Freitas, S.C., Trigo, I.F., Macedo, J., Barroso, C., Silva, R., and Perdigão, R. (2013). Land surface temperature from multiple geostationary satellites. International Journal of Remote Sensing, 34 (9-10): 3051-3068.

[28]. Gohain, K.J., Mohammad, P., and Goswami, A. (2021). Assessing the impact of land use land cover changes on land surface temperature over Pune city, India. Quaternary International, 575, 259-269.

[29]. Kalma, J.D., McVicar, T.R., and McCabe, M.F. (2008). Estimating land surface evaporation: A review of methods using remotely sensed surface temperature data. Surveys in Geophysics, 29 (4): 421-469.

[30]. Kumar, D. and Shekhar, S. (2015). Statistical analysis of land surface temperature–vegetation indexes relationship through thermal remote sensing. Ecotoxicology and environmental safety, 121, 39-44.

[31]. Mallick, J., Kant, Y., and Bharath, B.D. (2008). Estimation of land surface temperature over Delhi using Landsat-7 ETM+. J. Ind. Geophys. Union.

[32]. Mumtaz, F., Tao, Y., de Leeuw, G., Zhao, L., Fan, C., Elnashar, A. and Wang, D. (2020). Modeling spatio-temporal land transformation and its associated impacts on land surface temperature (LST). Remote Sensing.

[33]. Ottlé, C. and Vidal-Madjar, D. (1992). Estimation of land surface temperature with NOAA9 data. Remote Sensing of Environment.

[34]. Parastatidis, D., Mitraka, Z., Chrysoulakis, N., and Abrams, M. (2017). Online global land surface temperature estimation from Landsat. Remote sensing.

[35]. Peng, X., Wu, W., Zheng, Y., Sun, J., Hu, T., and Wang, P. (2020). Correlation analysis of land surface temperature and topographic elements in Hangzhou, China. Scientific Reports.

[36]. Qiao, Z., Liu, L., Qin, Y., Xu, X., Wang, B., and Liu, Z. (2020). The impact of urban renewal on land surface temperature changes: a case study in the main city of Guangzhou, China. Remote Sensing.

[37]. Rozenstein, O., Qin, Z., Derimian, Y., and Karnieli, A. (2014). Derivation of land surface temperature for Landsat-8 TIRS using a split window algorithm. Sensors.

[38]. Singh, P.K., Gaur, M.L., Mishra, S.K., and Rawat, S.S. (2010). An updated hydrological review on recent advancements in soil conservation service-curve number technique. Journal of Water and Climate Change, 1 (2): 118-134.

[39]. Sun, D. and Pinker, R.T. (2003). Estimation of land surface temperature from a Geostationary Operational Environmental Satellite (GOES-8). Journal of geophysical research: atmospheres, 108(D11).

[40]. Sun, Q., Wu, Z., and Tan, J. (2012). The relationship between land surface temperature and land

use/land cover in Guangzhou, China. Environmental Earth Sciences, 65 (6): 1687-1694.

[41]. Tomlinson, C.J., Chapman, L., Thornes, J.E., and Baker, C. (2011). Remote sensing land surface temperature for meteorology and climatology: A review. Meteorological Applications, 18 (3): 296-306.

[42]. Wan, Z. (2014). New refinements and validation of the collection-6 MODIS land-surface temperature/emissivity product. Remote sensing of Environment, 140, 36-45.

[43]. Xu, Y. and Shen, Y. (2013). Reconstruction of the land surface temperature time series using harmonic analysis. Computers & geosciences, 61, 126-132.

[44]. Yang, J., Ren, J., Sun, D., Xiao, X., Xia, J.C., Jin, C., and Li, X. (2021). Understanding land surface temperature impact factors based on local climate zones. Sustainable Cities and Society, 69, 102818.

تخمین دمای سطح زمین در منطقه‌ی صاحب زاده آجیت سینگ ناگار، پنجاب، هند

کاوستوب سینها، پریانگی شارما، کانوارپریت سینگ*، سوشیندرا کومار گوپتا و آبیشک شارما

گروه مهندسی عمران، دانشگاه چندیگر، غروان، پنجاب، هند

ارسال 2023/04/05، پذیرش 2023/05/02

* نویسنده مسئول مکاتبات: Kanwarpreet.e9570@cumail.in

چکیده:

دمای سطح زمین (LST) یکی از مهمترین ویژگی‌های زمین شناسی هر منطقه در عصر حاضر است. در طول مطالعه، اطلاعات مربوط به دمای سطح زمین با استفاده از نرم افزار Arc-GIS محاسبه شده است. برای محاسبه LST از تصاویر ماهواره‌ای LANDSAT 8 (2022) و LANDSAT 4-5 (2001 و 2011) استفاده می‌شود. از نقشه‌های LST سال‌های 2001 و 2011، افزایش قابل توجهی مشاهده شده است. این امر به دلیل افزایش سریع جمعیت در منطقه مذکور است. یک افزایش تدریجی در LST بین دوره دوم 2011-2022 وجود دارد. ارتباط بین LST و رطوبت خاص نیز در این جنبه ترسیم شده است. رطوبت ویژه منطقه در بازه زمانی مورد نظر افزایش چشمگیری داشته است. به طور کلی، مشاهده می‌شود که LST منطقه به سرعت از حداقل دمای 12 درجه سانتیگراد در سال 2001 به 27 درجه سانتیگراد در سال 2022 افزایش یافته است. این به دلیل فعالیت‌های انسانی در منطقه است که در نهایت به تخریب شرایط اقلیمی و محیطی مانند LST کمک کرده است.

کلمات کلیدی: LST، NDVI، دمای روشنایی، PV، رطوبت خاص.